Generalizing the fractal model of soil structure: the pore–solid fractal approach

Edith Perrier [a,1], Nigel Bird [b,2], Michel Rieu [a,*]

[a] *ORSTOM, Laboratoire d'Informatique Appliquée, 32 av. Henri Varagnat, 93143 Bondy Cedex, France*
[b] *Silsoe Research Institute, Soil Science Group, Wrest Park Silsoe, Bedford MK45 4HS, UK*

Abstract

We review a generalized approach to modeling soil structures, which exhibit scale invariant, or self-similar local structure over a range of scales. Within this approach almost all existing fractal models of soil structure feature as special albeit degenerate cases. A general model is considered which is shown to exhibit either a fractal or nonfractal pore surface depending on the model parameters. With the exception of two special cases corresponding to a solid mass fractal and a pore mass fractal the model displays symmetric power law or fractal pore size and solid size distributions. In this context the model provides an example of a porous structure in which pore sizes can be inferred from associated solid particle sizes through this symmetry. Again with two exceptions the model is shown to exhibit scaling of solid and pore volumes as a function of the resolution of measurement contrary to that of a mass fractal structure and to possess porosity other than zero or unity when local structure is included at arbitrarily small scales contrary to the situation arising in the case of a solid mass fractal and a pore mass fractal model respectively. Consequently the model not only generalizes the fractal approach to modeling soil structure but introduces properties central to the characterization of a soil which are quite distinct from those exhibited by existing fractal models. The model thus offers a wider scope for modeling self-similar multiscale soil structures than that currently operating. © 1999 Elsevier Science B.V. All rights reserved.

Keywords: fractal; soil structure; pore surface; pore mass

_____

[*] Corresponding author. E-mail: rieu@paris.orstom.fr
[1] E-mail: perrier@bondy.orstom.fr
[2] E-mail: bird@bbsrc.ac.uk

1. Introduction

Fractals are becoming increasingly popular in soil physics research as a means for characterizing various properties of porous media. They have been used both in theoretical and practical studies to model: (i) fractal number–size distributions (pore size distributions: Friesen and Mikula, 1987; Ahl and Niemeyer, 1989; Tyler and Wheatcraft, 1990; Rieu and Sposito, 1991c; Perrier et al., 1996; particle size distributions: Tyler and Wheatcraft, 1989, 1992; Wu et al., 1993); (ii) fractal surfaces (pore–solid interface: Pfeifer and Avnir, 1983, de Gennes, 1985, Friesen and Mikula, 1987; Davis, 1989, van Damme and Ben Ohoud, 1990; Toledo et al., 1990; Bartoli et al., 1991; Crawford et al., 1995) and (iii) mass fractal properties (solid mass fractal: Friesen and Mikula, 1987; Bartoli et al., 1991; Rieu and Sposito, 1991c; Young and Crawford, 1991; Crawford, 1994; Bird et al., 1996; Crawford et al., 1995; Perrier et al., 1995; or associated aggregate distributions: Perfect and Kay, 1991; Crawford et al., 1993; or pore mass fractal: Katz and Thompson, 1985; Ghilardi et al., 1993). The main purpose of these studies is to analyze or characterize complex multiscale porous structures. As far as soil structure is concerned, attention to date has focused mainly on modeling soil structures and, in particular, soil aggregate structures in terms of solid mass fractals and on modeling the pore–solid interface within the soil in terms of fractal surfaces. The essential feature common to each fractal model is scale invariance, that is the structure in question is composed of parts which appear similar to the whole. Examples include the now familiar Menger sponge (or Sierpinski carpet) in the context of a mass fractal model and the Von Koch curve, or the internal surface of a Menger sponge in the context of a fractal surface model. Our purpose is to review a new approach to modeling multiscale porous media and soil structures in particular. This involves an alternative class of models which can be viewed as a generalization of the previously quoted fractal models. Like any fractal model, the new class exhibits self-similar properties. In other important respects, central to the characterization of a porous medium, it is quite distinct. We will call it a 'pore–solid fractal' model (PSF).

The PSF model originates from two studies. Neimark (1989) developed the 'self-similar multiscale percolation system', a representation of a disordered, disperse medium that exhibits a fractal interface between solid and pore phases. Perrier (1994) independently proposed a multiscale model of soil structure which combines a fractal pore number–size distribution and a fractal solid number–size distribution. Although these two models have been developed in different contexts, using slightly different definitions, and presenting different local geometrical shapes, they are nevertheless equivalent in terms of the features considered in this paper. After a quick review of the principles of modelling a fractal porous medium we will define the PSF model within this conceptual framework using Neimark's definition. Equivalence with Perrier's

definition is given in Appendix A. First we will show how the PSF model actually gathers in a single structure the previous properties of fractal pore and solid number–size distributions and a pore–solid fractal interface. Then we will examine further properties of the PSF model: we will show that it combines in a geometrical pattern pores and solids at any stage of its development, and we will derive its scaling properties as regards the solid or pore mass, showing that a PSF in its general form is not a mass fractal. Finally, in Section 4, we will see that the PSF model reduces to a classic solid or pore mass fractal in two symmetric limiting cases, and, more generally, that the PSF model constitutes a general framework for analysing and comparing most of the previous fractal models of porous structures in soil science.

2. Fractal objects

2.1. Basic construction

Construction of a deterministic self-similar fractal object of fractal dimension D, embedded in an Euclidean space of dimension d, is based on the following: First, an initiator (Fig. 1a) which defines a region of linear size L in a space of Euclidean dimension d. This region can be divided into N equal parts or subregions of linear size L/n paving the whole object. Second, a generator (Fig. 1b) which (i) divides the N parts into two sets of Nz (shown in light gray in
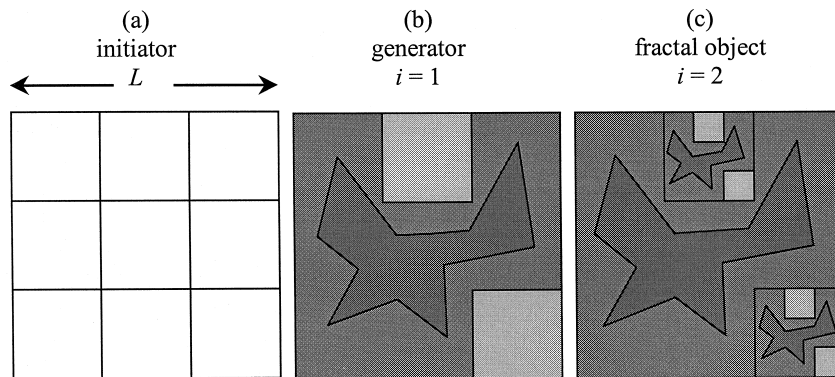
$$d = 2, \ n = 3, \ z = 2/9, \ D = \log 2/\log 3 = 0.631, \ Nz = 2$$

Fig. 1. Basic construction of a fractal object. In a space of Euclidean dimension d, the initiator (a) defines a region of linear size L divided into N equal parts. At the first iteration step, the generator (b) divides the N parts into two sets of Nz (light gray) and $N(1-z)$ (dark gray) subregions, determines the location of the Nz subregions and defines a pattern inside the $N(1-z)$ subregions. At the next step, each of the Nz subregions is replaced by a reduced replicate of the generator.

Fig. 1b) and $N(1-z)$ (shown in dark gray in Fig. 1b) subregions ($z < 1$); (ii) defines a pattern inside the $N(1-z)$ subregions; (iii) defines the location of the Nz subregions where the whole shape will be replicated.

Then a recursive process replaces each of the Nz subregions by the generator reduced by the same ratio $1/n$ (Fig. 1c for step 2) and so forth at subsequent steps i.

2.2. General properties

The smaller subregions pave the whole initiator so that $N(L/n)^d = L^d$, that is

$$N = n^d \tag{1}$$

The fractal dimension D follows from the number of replicates and the similarity ratio by

$$D = \frac{\log(Nz)}{\log(n)}. \tag{2}$$

Eq. (2) may be rearranged as:

$$Nz = n^D. \tag{3}$$

Combining Eqs. (1) and (3) we obtain

$$z = n^{D-d}, \tag{4}$$

and

$$nz = n^{D-(d-1)}. \tag{5}$$

Let $\mathcal{N}_z(r_i)$ be the number of replicates of size r_i created at each step i of the development of the structure. r_i is defined by

$$r_i = L(n)^{-i} \quad \text{or} \quad n^i = L/r_i. \tag{6}$$

The number of replicates created at step 1 is: $\mathcal{N}_z(r_1) = Nz$.

At the next iteration step, Nz replicates of size r_2 are created in each replicate of size r_1. Then at step i,

$$\mathcal{N}_z(r_i) = (Nz)\mathcal{N}_z(r_{i-1}) = Nz(Nz)^{i-1}.$$

or

$$\mathcal{N}_z(r_i) = (Nz)^i. \tag{7}$$

Using Eqs. (3) and (6) we obtain

$$(Nz)^i = (n^D)^i = (n^{-i})^{-D} = (L^{-1}r_i)^{-D} = L^D r_i^{-D}, \tag{8}$$

and

$$\mathcal{N}_z(r_i) = L^D r_i^{-D}. \tag{9}$$

Eq. (9) expresses the relationship between the number of replicates and their size as a power law function with an exponent equal to $-D$, where D is the fractal dimension.

In a similar way, several parameters of the fractal object can also be expressed as power law functions of the resolution scale r_i. Formulas (10) to (12) will be useful in further derivations:From Eqs. (1) and (6)

$$N^i = L^d r_i^{-d}. \tag{10}$$

From Eqs. (4) and (6)

$$z^i = L^{D-d} r_i^{d-D}. \tag{11}$$

From Eqs. (5) and (6)

$$(nz)^i = L^{D-(d-1)} r_i^{(d-1)-D}. \tag{12}$$

2.3. Classical ways to model a porous medium

Depending on the modeling context, the $N(1-z)$ subregions may represent different patterns. When fractal objects are used to model porous media made of a solid phase and a pore phase, the set of these $N(1-z)$ subregions represents generally an homogeneous material (shown in dark gray in Fig. 2) rather than a heterogeneous one (Fig. 1).

generator ($i = 1$)   fractal object ($i = 2$)
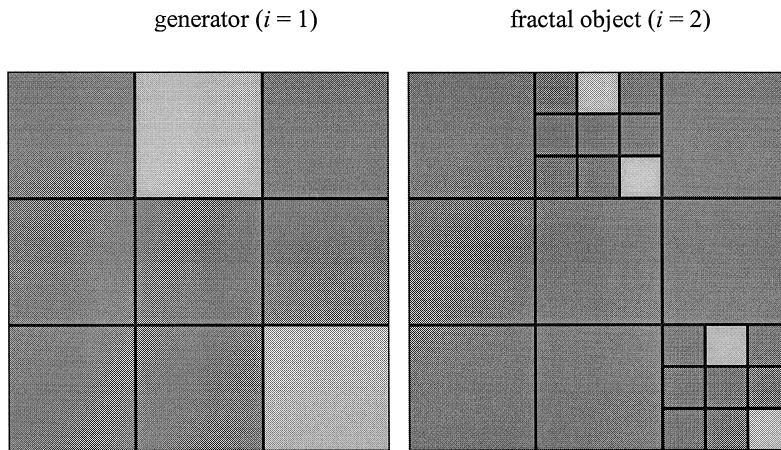
$d = 2, n = 3, z = 2/9, D = 0.631$

Fig. 2. The first two steps of the development of a fractal porous medium. The $N(1-z)$ (dark gray) subregions are associated with an homogeneous material.

(a)   (b)

(1)
generator ($i = 1$)

(2)
second step ($i = 2$)

(3)
if $i \to \infty$

(4)
if last step $m = 4$
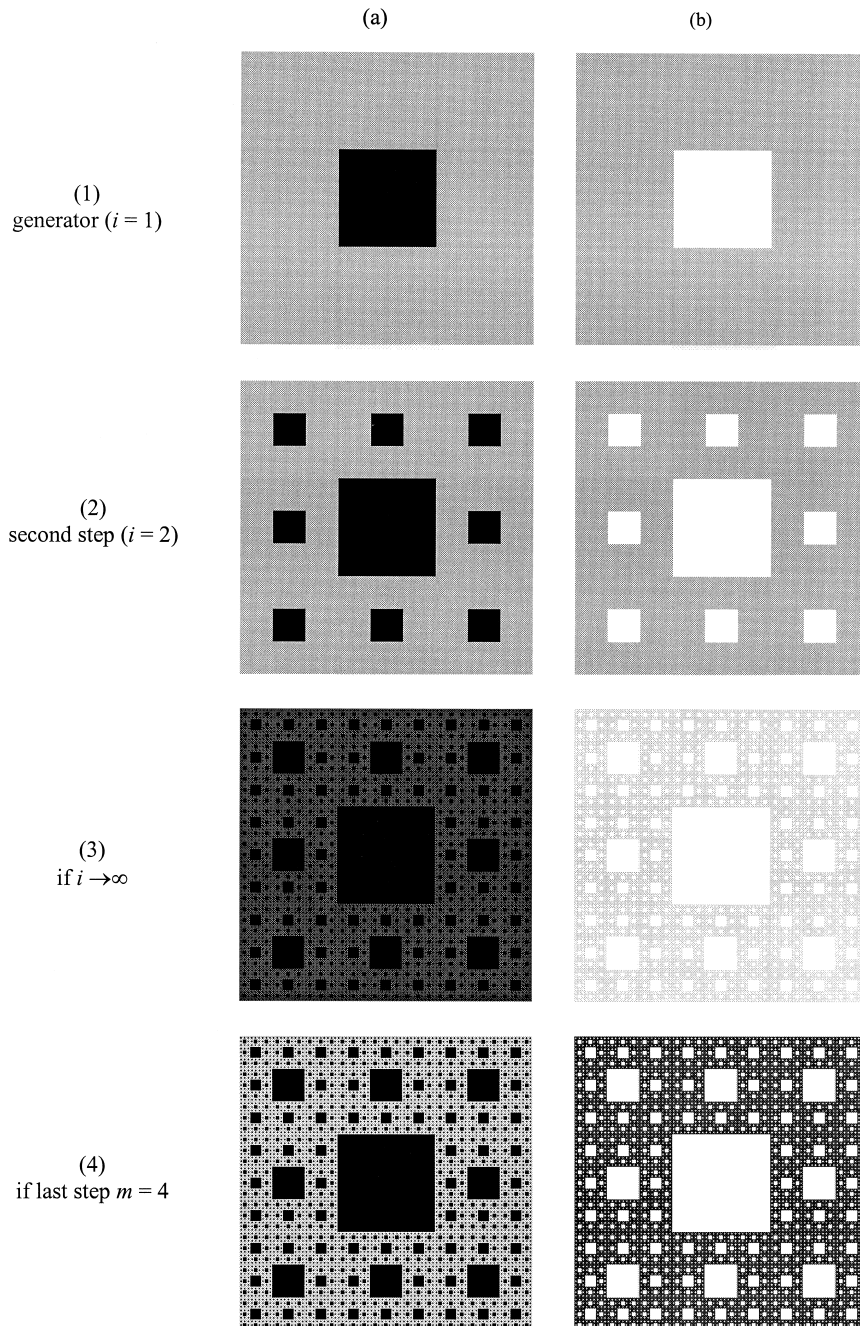
$d = 2, n = 3, z = 8/9, D = 1.893$

This homogeneous material can be identified either with the solid phase of the porous medium (shown in black in Fig. 3a.1) ('pore mass fractal') or the pore phase (shown in white in Fig. 3b.1) ('solid mass fractal').

At each step i, reduced copies of the generator in the Nz subregions (shown in light gray in Fig. 3a.1) reveal new details at finer resolution scales (Fig. 3a.2 and b.2). These subregions constitute the 'fractal set'.

Two main options have been considered in previous studies: (i) Iterations are carried out ad infinitum, and the fractal set of $(Nz)^i$ subregions vanishes. The model represents only solid in the so-called pore mass fractal (Fig. 3a.3) or only pores in the solid mass fractal (Fig. 3b.3). (ii) A lower cutoff of scale is assumed, considering a finite number of recursive iterations m. The $(Nz)^m$ subregions created at the last iteration step $i = m$ will undergo no further division and the fractal set is assumed to model the complementary phase: in a pore mass fractal it is associated with the pore phase (shown in very light gray in Fig. 3a.4), and in a solid mass fractal it is associated with the solid phase (shown in black in Fig. 3b.4).

3. The PSF model

3.1. Definition

Following the approach of Neimark, which combines pores and solids in the model in an interesting symmetrical setting, we define the $(1 - z)$ proportion of the generator as a mixture of pore and solid defined as follows:

$$(1 - z) = (x + y) \tag{13}$$

where x denotes the proportion of pore phase, y the proportion of solid phase and z represents the proportion of the generator where the whole shape is replicated at each step. Solids and pores generated at each step are kept whereas the fractal set is transformed (Fig. 4).

Combining Eqs. (13), (1) and (2) we can express the fractal dimension as:

$$D = d + \frac{\log(1 - x - y)}{\log n} . \tag{14}$$

Eq. (14) shows that for a given Euclidean dimension d, the value of the fractal dimension D of a PSF model depends only on the value of parameters n, x and y.

Fig. 3. Classical example of a pore mass fractal (a) and a solid mass fractal (b) modeling a porous medium. The pore phase is shown in white or very light gray and the solid phase is shown in black. If infinite iterations are carried out, the pore mass fractal represents only solid (a.3) and the solid mass fractal only void (b.3). If a lower cutoff of scale is assumed, the fractal set (shown in light gray) is associated with the pore phase (a.4) or the solid phase (b.4).

generator ($i = 1$)   fractal object ($i = 2$)
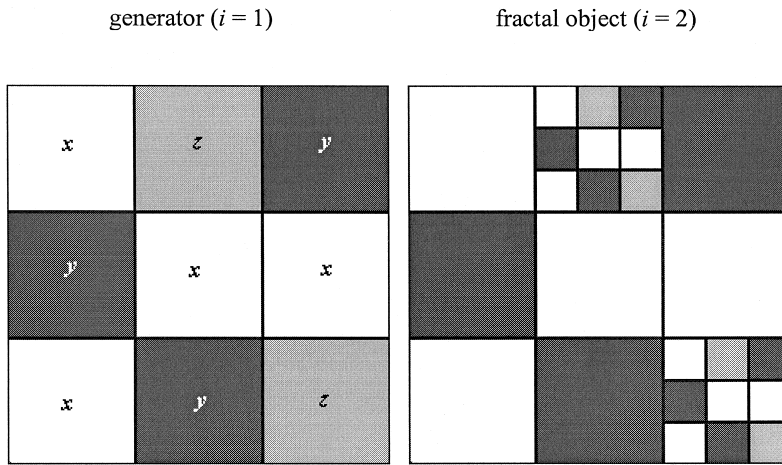
$d = 2,\ n = 3,\ z = 2/9,\ x = 4/9,\ y = 3/9,\ D = 2 + \log(1\text{-}7/9)/\log 3 = 0.631$

Fig. 4. Definition of a PSF model. The $N(1 - z)$ subregions are divided into $Nx = 4$ pore subregions (white) and $Ny = 3$ solid subregions (black). The fractal set (light gray) corresponds to $Nz = 2$ subregions where the whole shape is replicated at next iteration step.

Parameters x, y and z can be considered as probabilities ($x + y + z = 1$) and mathematical calculations can be done in a probabilistic way (Neimark, 1989). However, for sake of simplicity, we will consider here that x, y and z are proportions and Nx, Ny, Nz refer to the number of subregions of each type, to get simple proofs based only on counting.

3.2. Counting elements

At step 1, there are only elements of size L/n: Nx pores, Ny solids and Nz subregions where the whole shape will be replicated at the next step.

At step 2, some elements of size L/n are kept: Nx pores, Ny solids, whereas new elements of size $L(n)^{-2}$ are added: $Nx(Nz)$ pores, $Ny(Nz)$ solids, and $Nz(Nz)$ subregions where the whole shape will be replicated at the next step.

At step i, let $\mathcal{N}_x(r_i)$ and $\mathcal{N}_y(r_i)$ be the respective numbers of pores and solids of size r_i. Then

$$\mathcal{N}_x(r_i) = (Nx)\mathcal{N}_z(r_{i-1}) \quad \text{and} \quad \mathcal{N}_y(r_i) = (Ny)\mathcal{N}_z(r_{i-1}).$$

Using Eq. (7) we obtain

$$\mathcal{N}_x(r_i) = Nx(Nz)^{i-1}, \tag{15a}$$

and using Eq. (8),

$$\mathcal{N}_x(r_i) = \frac{Nx}{Nz}(Nz)^i = \frac{x}{z}L^D r_i^{-D}.$$ (15b)

In a symmetric way, we can write

$$\mathcal{N}_y(r_i) = Ny(Nz)^{i-1}$$ (16a)

or

$$\mathcal{N}_y(r_i) = \frac{Ny}{Nz}(Nz)^i = \frac{y}{z}L^D r_i^{-D}.$$ (16b)

More generally, the number of elements of size r_i added at each step scales as a power $-D$ of the size:

$$\mathcal{N}_x(r_i) \propto r_i^{-D}, \quad \mathcal{N}_y(r_i) \propto r_i^{-D}, \quad \mathcal{N}_z(r_i) \propto r_i^{-D}.$$ (17)

3.3. Porosity

Since x represents the proportion of pores kept at step 1 by the generator, zx is the proportion of pores added in the replicates generated at step 2, and so on. Thus the porosity ϕ_i at step i is the following sum:

$$\phi = x + zx + z^2 x + \ldots + z^{i-1}x = x\sum_{j=0}^{i-1} z^j = x\left(\frac{z^i - 1}{z - 1}\right).$$ (18)

From Eq. (13) we obtain

$$\phi_i = \frac{x}{x+y}(1 - z^i).$$ (19)

As the number of iterations i increases to infinity, $z^i \to 0$ and Eq. (19) becomes (cf. Neimark, 1989 and Perrier, 1994):

$$\phi = \frac{x}{x+y}$$ (20)

Eq. (20) shows that a PSF model exhibits a finite value of the total porosity which depends only on the value of parameters x and y.

3.4. Cumulative number–size distributions of pores and solids

It is commonly assumed that, when a collection of self-similar objects exhibits a cumulative number–size distribution of objects in the form:

$$N(r) \propto r^{-D}.$$ (21)

the collection may be called fractal of dimension D (Mandelbrot, 1983).

Let $N_x(r_i)$ and $N_y(r_i)$ be the respective numbers of pores and solids of size greater than or equal to r_i.

At iteration step $i = 1$, the number of pores is $N_x(r_1) = \mathcal{N}_x(r_1) = Nx$.

For $i = 2$, $N_x(r_2) = N_x(r_1) + \mathcal{N}_x(r_2) = Nx + Nx(Nz) = Nx(1 + Nz)$, and at any step i:

$$N_x(r_i) = N_x(r_{i-1}) + \mathcal{N}_x(r_i) = Nx\left(1 + Nz + (Nz)^2 + \ldots + (Nz)^{i-1}\right).$$

Summation of this geometric series of ratio Nz yields:

$$N_x(r_i) = Nx \sum_{j=0}^{i-1} (Nz)^j = Nx\left(\frac{(Nz)^i - 1}{Nz - 1}\right). \tag{22}$$

If $Nz > 1$, as $i \to \infty$, $(Nz)^i \gg 1$ and $((Nz)^i - 1) \cong (Nz)^i$. Using Eq. (8) one gets

$$N_x(r_i) \cong \frac{Nx}{Nz - 1}(Nz)^i = \frac{Nx}{Nz - 1}L^D r_i^{-D}. \tag{23a}$$

In a symmetric way, the cumulative number of solids greater than or equal to r_i is obtained by substituting x by y in Eq. (23a)

$$N_y(r_i) \cong \frac{Ny}{Nz - 1}(Nz)^i = \frac{Ny}{Nz - 1}L^D r_i^{-D}. \tag{23b}$$

Eqs. (23a) and (23b) are discrete analogs of Eq. (21). They can be rewritten as:

$$N_x(r_i) \propto r_i^{-D}, \tag{24a}$$

and

$$N_y(r_i) \propto r_i^{-D}. \tag{24b}$$

Eqs. (24a) and (24b) show the symmetry exhibited by the PSF model: both the pore number–size distribution and the solids number–size distribution assume a power law form with identical exponent $-D$, where D is the fractal dimension.

3.5. Pore–solid interface

Another fractal property commonly observed in some porous media is related to the measurement of the pore–solid interface.

A surface is called fractal of dimension D when its area $S(l)$ measured with units l^{d-1} scales as l^{d-1-D} where $d - 1 < D < d$, that is:

$$\frac{S(l)}{l^{d-1}} \propto l^{-D}. \tag{25}$$

Neimark (1989) has studied the properties of ''the surface of a self similar multiscale percolation system''. For completeness, we include here our own derivation of the interface behavior in a PSF model. The area $S(i)$ of the pore–solid interface (perimeter when $d = 2$, surface when $d = 3$) can be first approximated by summing the surfaces of all the boundaries of the solid elements which have been created after i iteration steps. These solid elements are squares $(d = 2)$ or cubes $(d = 3)$ of size greater than or equal to r_i. Each solid subregion of linear size r_i has a surface $2\,dr_i^{d-1}$ and the cumulative boundary of the solid elements, denoted $S_y(i)$ is equal to:

$$S_y(i) = \sum_{j=1}^{i} \left(\mathcal{N}_y(r_j) \right) \left(2\,dr_j^{d-1} \right). \tag{26}$$

Introducing Eqs. (16a) and (6), we obtain

$$S_y(i) = 2\,d \sum_{j=1}^{i} Ny(Nz)^{j-1} (Ln^{-j})^{d-1}, \tag{27}$$

$$S_y(i) = 2\,dNyL^{d-1} \sum_{j=1}^{i} (Nz)^{j-1} (n^{-(d-1)})^{j} = 2\,dNy \left(\frac{L}{n} \right)^{d-1} \sum_{j=1}^{i} \left(\frac{Nz}{n^{d-1}} \right)^{j-1}. \tag{28}$$

Using Eq. (1), we get

$$S_y(i) = 2\,dn^d y \left(\frac{L}{n} \right)^{d-1} \sum_{j=1}^{i} \left(\frac{n^d z}{n^{d-1}} \right)^{j-1} = 2\,dy \left(\frac{L}{n} \right)^{-1} L^d \sum_{j=1}^{i} (nz)^{j-1}. \tag{29}$$

The value of the geometric series in Eq. (29) depends on the value of nz. If $nz = 1$,

$$S_y(i) = 2\,dy \left(\frac{L}{n} \right)^{-1} L^d i. \tag{30}$$

From Eq. (6) we obtain $i = (\log L/r_i)/(\log n)$ and Eq. (30) becomes

$$S_y(i) = \frac{2\,dnyL^{d-1}}{\log n} \log \frac{L}{r_i}. \tag{31}$$

If $nz \neq 1$,

$$S_y(i) = 2\,dy \left(\frac{L}{n} \right)^{-1} L^d \frac{(nz)^i - 1}{nz - 1}. \tag{32}$$

From Eq. (12) we have $(nz)^i = L^{D-d+1}r_i^{d-1-D}$ and Eq. (32) becomes

$$S_y(i) = y\frac{2\,dnL^{d-1}}{1-nz} + y\frac{2\,dnL^D}{nz-1}r_i^{d-1-D}. \tag{33a}$$

In a symmetric way, the cumulative area of the boundaries of pores created at i iteration steps is given by

$$S_x(i) = x\frac{2\,dnL^{d-1}}{1-nz} + x\frac{2\,dnL^D}{nz-1}r_i^{d-1-D}. \tag{33b}$$

The actual interface $S(i)$ between solids and pores cannot be calculated so simply, because the location of the solid and pores subregions in the model must be taken into account. At each step i, we consider a constant number Ny (or Nx) of solid (or pore) subregions but randomly distributed in space. If two solid subregions have a common side, this side belongs to the total boundary measured by $S_y(i)$, but not to the solid–pore interface. Thus $S(i) < S_x(i)$ and $S(i) < S_y(i)$.

In a random realization, assuming $x \neq 0$, $y \neq 0$, the calculation of $S(i)$ can be done in a probabilistic manner. As the number of iterations increases to infinity, the fractal set of $(Nz)^i$ subregions vanishes and the probability $p_x(i)$ that an arbitrary chosen point on the solid boundary belongs to the interface is equal to the probability that the neighboring point outside the solid is located in a pore subregion. Thus as infinite iterations are carried out, $p_x(i) \to_{i\to\infty} \phi$, where ϕ is the porosity.

Then, using Eq. (19)

$$S(i) = p_x(i)S_y(i) = \phi S_y(i) = \frac{x}{x+y}S_y(i) \tag{34a}$$

or in a symmetrical way we could get

$$S(i) = p_y(i)S_x(i) = (1-\phi)S_x(i) = \frac{y}{x+y}S_x(i). \tag{34b}$$

and from Eqs. (33a) and (33b), Eqs. (34a) and (34b) are strictly identical.

Three cases must be distinguished.

(i) If $D = d - 1$ (that is $nz = 1$). From Eqs. (31) and (34a) we obtain

$$S(i) = \frac{xy}{x+y}\frac{2\,dnL^{d-1}}{\log n}\log\frac{L}{r_i}. \tag{35}$$

The surface of the solid–pore interface approaches infinity approximately as the logarithm of the inverse of r_i.

If $nz \neq 1$

(ii) if $D < d - 1$ (that is $nz < 1$).

Using Eqs. (33a) and (34a) we get

$$S(i) = \frac{x}{x+y} \left(\frac{2\, dynL^{d-1}}{1 - nz} + \frac{2\, dynL^{D}}{nz - 1} r_i^{d-1-D} \right) \tag{36a}$$

or from Eqs. (33b) and (34b)

$$S(i) = \frac{y}{x+y} \left(\frac{2\, dxnL^{d-1}}{1 - nz} + \frac{2\, dxnL^{D}}{nz - 1} r_i^{d-1-D} \right). \tag{36b}$$

As $i \to \infty$, $r_i \to 0$, $r_i^{d-1-D} \to 0$ thus

$$S(i) \xrightarrow[i \to \infty]{} \frac{xy}{x+y} \frac{2\, dnL^{d-1}}{1 - nz}. \tag{37}$$

The surface of the solid–pore interface approaches a finite value.

(iii) If $D > d - 1$ (that is $nz > 1$).

Eqs. (36a) and (36b) may be rewritten as

$$S(i) = \frac{xy}{x+y} \frac{2\, dnL^{d-1}}{1 - nz} + \frac{xy}{x+y} \frac{2\, dnL^{D}}{nz - 1} r_i^{d-1-D} \tag{38}$$

As $i \to \infty$, $r_i \to 0$, and $r_i^{d-1-D} \to \infty$. As the second term of the right side of Eq. (38) grows without limit, the first constant term becomes negligible. Thus

$$S(i) \xrightarrow[i \to \infty]{} \frac{xy}{x+y} \frac{2\, dnL^{D}}{nz - 1} r_i^{d-1-D}, \tag{39}$$

or (cf. Eq. (25)):

$$\frac{S(i)}{r_i^{d-1}} \xrightarrow[i \to \infty]{} C_1 r_i^{-D} \tag{40}$$

where C_1 is a constant. The area of the pore–solid interface approaches infinity as a power law function of the resolution scale. It is fractal of dimension D.

3.6. Mass of pores and solids

Fractal models often refer to so-called mass fractal properties, where the term mass actually means the solid or pore volume (the mass is proportional to the volume if a uniform density is assumed).

An object is called a mass fractal if the number $B(r)$ of boxes of size r needed to cover it scales as r^{-D}

$$B(r) \propto r^{-D} \tag{41a}$$

or if its mass $M(r)$ measured with units r^d scales as r^{-D}

$$\frac{M(r)}{r^d} \propto r^{-D}. \tag{41b}$$

In the PSF model, measuring mass with a box-counting method, let $B_y(i)$ be the number of boxes of size r_i needed to cover the volume of solids.

At the start, $B_y(0) = 1$ box of size $r_0 = L$ covers the whole structure.

At first step, $B_y(1) = Ny + Nz$ boxes of size r_i are needed to cover the solids.

At step 2, there are $B_y(2) = N(Ny) + NzB_y(1)$ boxes of size r_2, and at step i, there will be: $B_y(i) = N^i y + NzB_y(i-1)$ boxes of size r_i covering the volume of solids. We can show by recurrence that

$$B_y(i) = N^i y\left(\frac{z^i - 1}{z - 1}\right) + (Nz)^i \tag{42}$$

$$B_y(i) \quad = N^i y + NzB_y(i-1) = N^i y + Nz\left(N^{i-1}y\left(\frac{z^{i-1} - 1}{z - 1}\right) + (Nz)^{i-1}\right)$$

$$= N^i y + Nz\left(N^{i-1}y\left(\frac{z^{i-1} - 1}{z - 1}\right)\right) + (Nz)^i = N^i y\left(1 + z\left(\frac{z^{i-1} - 1}{z - 1}\right)\right) + (Nz)^i$$

$$= N^i y\left(\frac{z - 1 + z^i - z}{z - 1}\right) + (Nz)^i = N^i y\left(\frac{z^i - 1}{z - 1}\right) + (Nz)^i.$$

Thus

$$B_y(i) = N^i y\left(\frac{z^i - 1}{z - 1}\right) + (Nz)^i = \frac{N^i yz^i - N^i y + z(Nz)^i - (Nz)^i}{z - 1}$$

$$= \frac{(Nz)^i(y + z - 1) - N^i y}{z - 1}$$

or

$$B_y(i) = \frac{x(Nz)^i + N^i y}{1 - z},$$

and introducing Eq. (13)

$$B_y(i) = \frac{x}{x + y}(Nz)^i + \frac{y}{x + y}N^i. \tag{43}$$

Using Eqs. (8) and (10), Eq. (43) can be rewritten as

$$B_y(i) = \frac{y}{x + y}L^d r_i^{-d} + \frac{x}{x + y}L^D r_i^{-D}. \tag{44a}$$

In the same way, covering the pores needs a number $B_x(i)$ of boxes varying as

$$B_x(i) = \frac{x}{x + y}L^d r_i^{-d} + \frac{y}{x + y}L^D r_i^{-D}. \tag{44b}$$

The symmetric expressions for $B_x(i)$ and $B_y(i)$ assume the form of the sum of two power law functions of the box size r_i with exponents $-d$ and $-D$, where d is the Euclidean dimension and D the fractal dimension. We conclude that, in a PSF model, neither the solid phase nor the pore phase exhibit fractal scaling. The PSF in its general form is not a true mass fractal.

The volumes of pores and solids measured with resolution r_i, which we denote by $M_x(i)$ and $M_y(i)$ respectively follow immediately from Eqs. (44a) and (44b) as

$$M_x(i) = B_x(i)r_i^d = \frac{x}{x+y}L^d + \frac{y}{x+y}L^D r_i^{d-D}, \tag{45a}$$

$$M_y(i) = B_y(i)r_i^d = \frac{y}{x+y}L^d + \frac{x}{x+y}L^D r_i^{d-D}. \tag{45b}$$

If infinite iterations are carried out, $M_x(i)$ and $M_y(i)$ approach finite values

$$M_x(i) \rightarrow \frac{x}{x+y}L^d = \phi L^d, \tag{46a}$$

$$M_y(i) \rightarrow \frac{y}{x+y}L^d = (1-\phi)L^d, \tag{46b}$$

as required.

4. Discussion

4.1. A new, consistent geometric representation of a two-phase porous structure

Many attempts to model fractal properties of complex real porous media involve rather simple geometric figures: the Sierpinki carpet, the Menger sponge, the fractal cube considered by Rieu and Sposito and many types of fractal, lacunar models (see Rieu and Perrier, 1997, for a review). Several models of fractal surface have been first proposed based on the Von Koch curve (Pfeifer and Avnir, 1983) or similar shapes. These theoretical models generally represent only the pore–solid interface and their use to model soil structure is limited. Mass fractals constitute a great improvement in the sense that they closely associate both solid and pore phases in a geometrical frame. Two main types of mass fractal model are commonly used (Rieu and Perrier, 1997). Pore mass fractals exhibit a fractal pore 'mass' by introducing a fractal cumulative number–size distribution of elements identified with solids in a fractal set identified with the pore phase (Fig. 3a). Solid mass fractals exhibit a fractal solid mass by introducing a fractal cumulative number–size distribution of elements identified with pores in a fractal set identified with a solid phase (Fig. 3b). However it should be noted that if, as in a true mathematical fractal, infinite
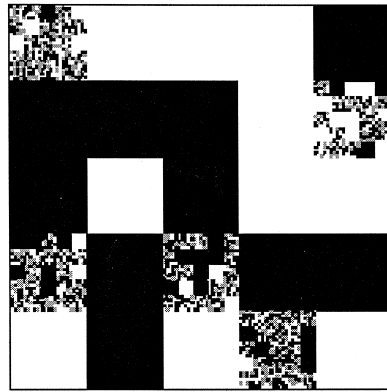
$d = 2, n = 5, z = 0.2, x = y = 0.4, D = 1, i = 3$

Fig. 5. Randomized PSF based on a square pattern. In this example, $D = 1$.

iterations are carried out in the recursive construction of the mass fractal, the pore space vanishes in pore mass fractals while the solid space vanishes in solid mass fractals. Paradoxically in this limit a pore mass fractal can represent a particle size distribution but no pores (Tyler and Wheatcraft, 1992, cf. Fig. 3a.3) and a solid mass fractal can represent a pore size distribution but no solids (Tyler and Wheatcraft, 1990, cf. Fig. 3b.3). Both may represent a purely theoretical fractal pore–solid interface, but neither in the limit is able to represent a two-phase porous medium.

Since it always associates in a single geometric shape two fractal cumulative number–size distributions of elements with a fractal set, the PSF model presented in this paper, is a more advanced fractal model of porous medium. Irrespective of the range of scale over which the structure is developed, both a solid phase and a pore phase are modelled by two power law distributions whereas the fractal set can be identified with either the solid or the pore phase if a lower cut-off of scale is considered or vanishes if infinite iterations are carried out (Figs. 5 and 6). This matter is not addressed by Neimark (1989) who was not interested in the properties of the solid whereas it is a central point of view in the approach of Perrier (1994).

A PSF and a mass fractal exhibit structure over a range of scales specified by the modeller. A well-known property of a solid mass fractal is that when this structure extends to arbitrarily small scales the porosity of the model approaches unity, assuming that the fractal set is identified with the solid phase and its complement is identified with the pore phase. When these identifications are reversed (pore mass fractal), the porosity approaches zero. These limiting values of porosity clearly have no physical relevance. This is in marked contrast to the porosity of the new model which is designed to attain limiting value of total
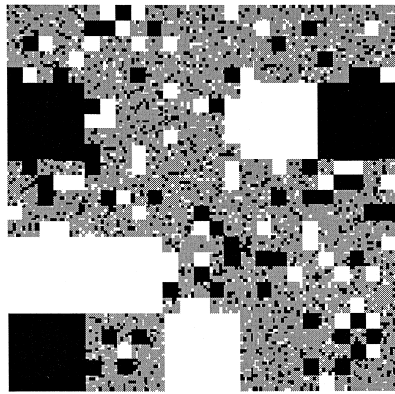
$$d = 2, n = 5, z = 0.72, x = y = 0.14, D = 1.796, i = 3$$

Fig. 6. Randomized PSF based on a square pattern. General case of $d - 1 \leq D < d$.

porosity ϕ lying between these two extremes and depending only on the values of the parameters x and y, that is the proportion of pore space and solid kept at each step. This peculiarity of PSF model is thus an important extension to the range of models available for modelling multiscale porous media and specifically soil structures.

4.2. The PSF model compared to classic mass fractal models

The scaling of the mass of solid or pores is a crucial point in modelling soil structures. This matter is not developed by Neimark (1989) neither by Perrier (1994), but the interesting scaling properties of a PSF deserve attention. A mass fractal possesses characteristic scaling properties which identify it as a fractal structure (see Rieu and Perrier, 1997 for a review). A PSF in its general form is not a mass fractal and its scaling properties are different. For a mass fractal a power law scaling relation is obtained from which the mass fractal dimension may be inferred. For a PSF, as shown by Eqs. (44a) and (44b), the corresponding relation assumes the form of the sum of an Euclidean power law function and a fractal power law function. Thus neither the solid mass nor the pore mass properly exhibit a fractal scaling. Whilst the scaling relations identify the PSF as a structure other than a mass fractal, it is important to note that it can nevertheless easily be confused with that of a mass fractal if it is examined over a narrow range of scales. Some degree of caution is thus required in the use of any algorithm to analyse soil data, and the theory suggests that some soils might have been called mass fractals on approximate grounds and might be better modelled by a PSF.

In the case $x = 0$, the PSF model reduces to a fractal number–size distribution of solids and a fractal set. If the latter is associated with the pore phase, the result is a pore mass fractal. From Eqs. (44a) and (44b) we then have that $B_y(i)$

exhibits Euclidean scaling while $B_x(i)$ exhibits fractal scaling as required. Similarly, if $y = 0$ and the fractal set is associated with the solid phase we obtain a solid mass fractal. Then Eqs. (44a) and (44b) show that $B_y(i)$ exhibits fractal scaling whilst $B_x(i)$ exhibits Euclidean scaling. Thus mass fractal models appear as degenerate cases of a PSF.

Both a PSF in its general form and a mass fractal exhibit self-similar properties in the sense that where local structure occurs, it is similar to the whole. The essential difference between the two which leads to the different scaling properties as shown above is that a PSF model is in places devoid of such local structure, whereas a mass fractal is not.

4.3. Pore and solid number–size distributions

In this paper, we use the expression 'solid' or 'solid element' instead of 'particle' or 'grain' used in other works (e.g., Haverkamp and Parlange, 1986). But we do not mean 'solid, porous aggregate' in the sense of Rieu and Sposito (1991a,b) or Crawford et al. (1995). We clarify this statement by noting that we identify 'particles' with the primary elements of a soil structure. The number–size distribution of solids and pores differ significantly between a mass fractal and a PSF. If a lower cut-off of scale is considered, in a solid mass fractal, i.e., a fractal set identified with the solid phase, the solids are of equal size (cf. Bird et al., 1996), whilst the complementary pore space exhibits a power law number–size distribution of pores, with a power law exponent equal to $-D$. Similarly for a pore mass fractal, i.e., a fractal set identified with the pore phase, the pores are of equal size while the solids size distribution is power law. In contrast, in a PSF symmetry exists between the pore-size and solid-size distributions. Specifically both distributions assume a power law form with identical power law exponent $-D$ (cf. Perrier, 1994), where D is the fractal dimension of the pore–solid interface. The existence of such a symmetry is interesting in relation to the established view that solid-size distributions convey information relating to porosity and pore–size distributions and consequently soil hydraulic properties, through relations which map known solid sizes onto inferred pore sizes (e.g., Arya and Paris, 1981; Haverkamp and Parlange, 1986). A PSF provides an example of a porous material where this view appears to some extent valid. Also of interest are previous suggestions that power law fractal pore-size and particle-size distributions can coexist within a soil (e.g., Tyler and Wheatcraft, 1992, who acknowledged that ''a theoretical development is not yet available''). Again a PSF, in contrast to a mass fractal, provides an explicit example of one such model where this situation occurs.

4.4. Pore–solid interface

In a mass fractal the pore–solid interface is the boundary between the solid (or the pores) distributed in the fractal pore (or solid) mass. This surface grows

as a power law of the resolution scale. It is fractal of dimension D. When the fractal structure is developed ad infinitum, the fractal pore (or solid) mass vanishes and the interface has no physical relevance. However, if a lower cut-off of scale is used, the area of the interface has a finite value and the fractal surface can model a real solid–pore interface. Neimark (1989) has shown that in his 'self-similar multiscale percolation system' both fractal and nonfractal surfaces can arise depending on the value of nz and consequently D. When a fractal surface occurs, this D is also the dimension of the surface. In our own derivation of the scaling behavior of the interface, based on the number–size distribution, we obtain the same result. Because it always associates both solid and pore phases, the PSF model exhibits a pore–solid interface even if the structure is developed towards infinity. Depending on the value of the fractal dimension, the area of the interface assume the form of a logarithmic function of the length scale r_i (in the case of $D = d - 1$, cf. Eq. (35)), or of a fractal power law ($D > d - 1$; cf. Eq. (39)), or it tends towards a constant finite value (for $D < d - 1$; cf. Eq. (37)).

It follows from the above that whilst a porous material can exhibit self-similar properties and fractal number–size distributions of its elements (pores, solids or both) this does not imply a fractal surface. This only occurs when $D > d - 1$ (see e.g., Pfeifer and Avnir, 1983; Friesen and Mikula, 1987; Toledo et al., 1990). Here mathematical calculation of the area of the interface brings evidence of this critical value $d - 1$. Fig. 5 presents the particular case of a PSF model with a fractal dimension $D = d - 1$. It is interesting to note that although not visually obvious, the solid–pore interface is not fractal in this instance as it

Table 1
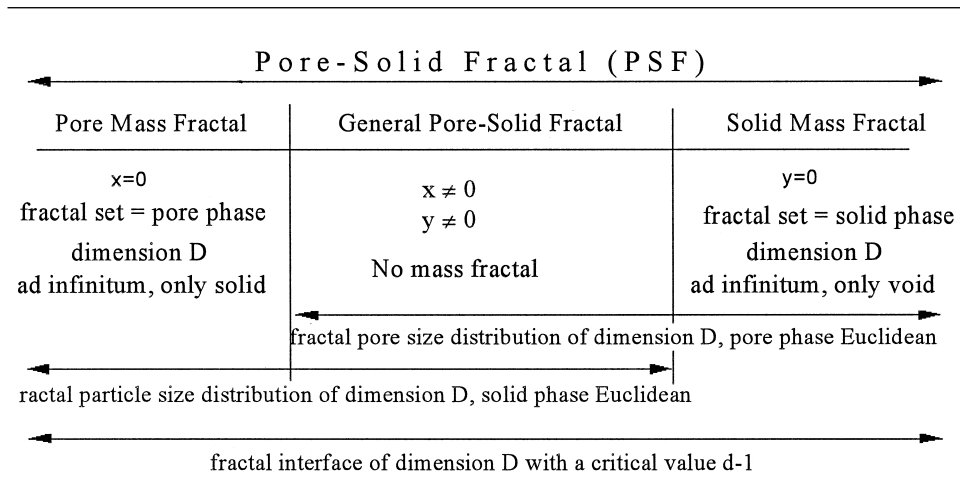Scaling properties of the PSF model and of pore and solid mass fractal models

Pore-Solid Fractal (PSF)		
Pore Mass Fractal	General Pore-Solid Fractal	Solid Mass Fractal
x=0 fractal set = pore phase dimension D ad infinitum, only solid	x ≠ 0 y ≠ 0 No mass fractal	y=0 fractal set = solid phase dimension D ad infinitum, only void

fractal pore size distribution of dimension D, pore phase Euclidean

ractal particle size distribution of dimension D, solid phase Euclidean

fractal interface of dimension D with a critical value d-1

Table 2
Summary of the features of the PSF model

PSF model parameters: [x→pore sub-regions] [y→solid sub-regions] [z→fractal set] [1/n = similarity ratio]	Pore Mass Fractal	General PSF	Solid Mass Fractal
	$x = 0$	$x \neq 0, y \neq 0$	$y = 0$
Basic relations (Equations 1 & 13)	$N = n^d$ $1 - z = y$	$N = n^d$ $1 - z = x + y$	$N = n^d$ $1 - z = x$
Fractal dimension (Equation 14)	$D = d + \dfrac{\log(1-y)}{\log n}$	$D = d + \dfrac{\log(1-x-y)}{\log n}$	$D = d + \dfrac{\log(1-x)}{\log n}$
Total porosity (Equation 20)	$\phi = 0$	$\phi = \dfrac{x}{x+y}$	$\phi = 1$
Number-size distribution of pores (Equation 23a)	none	$N_x(r_i) \cong \dfrac{Nx}{Nz-1} L^D r_i^{-D}$	$N_x(r_i) \cong \dfrac{Nx}{Nz-1} L^D r_i^{-D}$
Number-size distribution of solids (Equation 23b)	$N_y(r_i) \cong \dfrac{Ny}{Nz-1} L^D r_i^{-D}$	$N_y(r_i) \cong \dfrac{Ny}{Nz-1} L^D r_i^{-D}$	none

	If fractal set $(Nz)^i \equiv$ pores		If fractal set $(Nz)^i \equiv$ solids
Mass of pores (Equations 8 & 45a)	$\dfrac{M_z(i)}{r_i^d} = (Nz)^i = L^D r_i^{-D}$	$\dfrac{M_x(i)}{r_i^d} = \dfrac{x}{x+y} L^d r_i^{-d} + \dfrac{y}{x+y} L^D r_i^{-D}$	$\dfrac{M_x(i)}{r_i^d} = L^d r_i^{-d}$
Mass of solids (Equations 45b & 8)	$\dfrac{M_y(i)}{r_i^d} = L^d r_i^{-d}$	$\dfrac{M_y(i)}{r_i^d} = \dfrac{y}{x+y} L^d r_i^{-d} + \dfrac{x}{x+y} L^D r_i^{-D}$	$\dfrac{M_z(i)}{r_i^d} = (Nz)^i = L^D r_i^{-D}$
Pore-solid interface	If fractal set $(Nz)^i \equiv$ pores	No condition on fractal set $(Nz)^i$	If fractal set $(Nz)^i \equiv$ solids
$D = d-1$ (Equation 35)	$r_i > 0$ $\quad S_y(i) = y \dfrac{2dnL^{d-1}}{\log n} \log \dfrac{L}{r_i}$	No limitation on r_i $\quad S(i) = \dfrac{xy}{x+y} \dfrac{2dnL^{d-1}}{\log n} \log \dfrac{L}{r_i}$	$r_i > 0$ $\quad S_x(i) = x \dfrac{2dnL^{d-1}}{\log n} \log \dfrac{L}{r_i}$
$D < d-1$ (Equations 33 & 37)	$S_y(i) = y \dfrac{2dnL^{d-1}}{1-nz} + y \dfrac{2dnL^D}{nz-1} r_i^{d-1-D}$	$S(i) \xrightarrow[i\to\infty]{} \dfrac{xy}{x+y} \dfrac{2dnL^{d-1}}{1-nz}$	$S_x(i) = x \dfrac{2dnL^{d-1}}{1-nz} + x \dfrac{2dnL^D}{nz-1} r_i^{d-1-D}$
$D > d-1$ (Equations 33 & 39)	$S_y(i) = y \dfrac{2dnL^{d-1}}{1-nz} + y \dfrac{2dnL^D}{nz-1} r_i^{d-1-D}$	$S(i) \xrightarrow[i\to\infty]{} \dfrac{xy}{x+y} \dfrac{2dnL^D}{nz-1} r_i^{d-1-D}$	$S_x(i) = x \dfrac{2dnL^{d-1}}{1-nz} + x \dfrac{2dnL^D}{nz-1} r_i^{d-1-D}$

grows in a logarithmic fashion when the structure is developed. Apart from the relatively small extension of the fractal set, nothing points out why the area of the solid–pore interface is on the critical point between a nonfractal surface whose area tends towards a finite constant value and a fractal surface whose area tends towards infinity when the structure is developed ad infinitum (Fig. 6).

Calculations of the area of the interface have been derived for $x \neq 0$, $y \neq 0$. Fig. 3 gives an illustration of the limiting cases $x = 0$, $y = 0$. When $x = 0$, the PSF becomes a pore mass fractal combining a fractal distribution of solids and a fractal set. Now if the supplementary assumption is made that the fractal set of $(Nz)^i$ subregions represent pores we can still define and measure a pore–solid interface. Symmetrically a pore–solid interface can be defined when $y = 0$. The general results concerning the fractal character of the pore–solid interface hold in these limiting cases.

4.5. Summary

The scaling properties of the PSF model are summarized in Table 1. It can be observed how the PSF is a generalization of mass fractal which may be viewed as special albeit degenerate case. Thus the PSF model can be used in many cases for the following purposes.

1. Either to represent soils which have been shown to be surface fractals, in the same way as simple surface models have already been used (e.g., Pfeifer and Avnir, 1983; de Gennes, 1985).

2. Or to represent soils which exhibit a fractal pore size distribution, in the same way as simple lacunar fractal models have already been used (e.g., Tyler and Wheatcraft, 1990; Rieu and Sposito, 1991a).

3. Or to represent soils which exhibit a fractal solid size distribution, in the same way as simple models of fractal number–size distributions have already been used (e.g., Tyler and Wheatcraft, 1992; Wu et al., 1993)

4. Or to represent soils which exhibit a fractal solid mass, in the same way as simple models of a fractal solid phase have already been used (e.g., Rieu and Sposito, 1991a; Young and Crawford, 1991).

5. Or to represent soils which exhibit a fractal pore mass, in the same way as simple models of a fractal pore phase have already been used (e.g., Katz and Thompson, 1985; Ghilardi et al., 1993).

In addition, because the PSF model is a self-consistent geometric model of the whole porous structure, whatever the particular fractal property it has be designed to model, it gives also information about the possible scaling behaviour of the other properties of the porous structure (cf. Table 2). For example, if we consider a soil exhibiting a fractal pore size distribution (Perrier et al., 1996), the PSF model suggests which properties of the solid phase and which hydraulic properties could be associated to this particular pore size distribution.
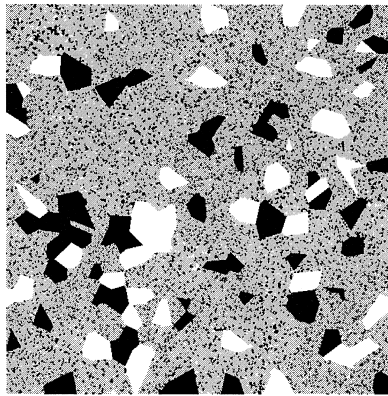
$d = 2, n = 20, z = 0.75, x = y = 0.125, D = 1.904, i = 2$

Fig. 7. Randomized PSF based on a polyedral pattern, with a division process obtained by a Voronoï tessellation. General case of $d - 1 \leq D < d$.

4.6. Extension: effect of different local geometric patterns

The ability of a fractal model of porous medium to represent a soil structure depends on its structural features: number–size distribution of its components, porosity, fractal scaling of the pore and solid phases, fractal scaling of the pore–solid interface, and on the behaviour ad infinitum of these properties. But this ability also depends strongly on the geometric patterns of the model. As an example, two realizations of the PSF model are presented Figs. 6 and 7. The first one is based on a square pattern. In the second, the division of the initiator is obtained by a Voronoï tessellation process (Perrier, 1994) and the basic pattern is polyhedral. In both cases, the proportions x, y and z have a constant value and the location of the pore and solid subregions is randomly determined at each iteration step. At any stage of its development, both structures exhibit the same properties: total porosity value lying between 0 and 1, fractal number–size distribution of pores and solids, nonfractal scaling of the pore and solid phases and fractal scaling of the pore–solid interface.

Improved geometric patterns may help in the construction of more realistic models of soil structure. As an example Figs. 8 and 9 present structures equivalent respectively to those presented in Figs. 6 and 7 in terms of their basic properties, but here the pores are located around the solids. Instead of keeping Ny solids and Nx pores among the $N(1 - z)$ subregions, an homothetic reduction of ratio k replaces each subregion of size r_i^d among the $N(1 - z)$ ones by one solid of size $k^d r_i^d$ surrounded by one pore of size $(1 - k^d)r_i^d$. This pattern proposed by Perrier (1994) is defined by a set of three parameters (N, z and k) whereas Neimark's percolation system and PSF model use (N, x and y). Equivalence between these two approaches is given in Appendix A.
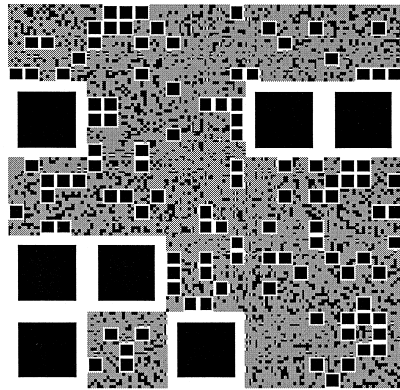
$d = 2, n = 5, z = 0.72, x = y = 0.14, D = 1.796, k = 0.707, i = 3$

Fig. 8. PSF numerically equivalent to the example presented in Fig. 6. Here, the void phase is located around the solid, resulting in a very different shape.

Obviously, some of these examples resemble soil structures more than others. In particular, each of them exhibits a specific kind of pore connectivity. As an illustration of this latter, Fig. 10 presents a mass fractal variation of the Sierpinski Carpet carried out by Perrier (1994). This degenerate form of PSF model is a 2D representation of a random realization of the fractal cube considered by Rieu and Sposito (1991a), fragmented by a Voronoï tessellation (Perrier et al., 1995). This fractal object is a solid mass fractal where a fractal cumulative number–size distribution of fractures is associated with a solid phase that exhibits a fractal scaling. As in the model presented in Fig. 3b, when this structure extends to arbitrarily small scales its porosity approaches unity.
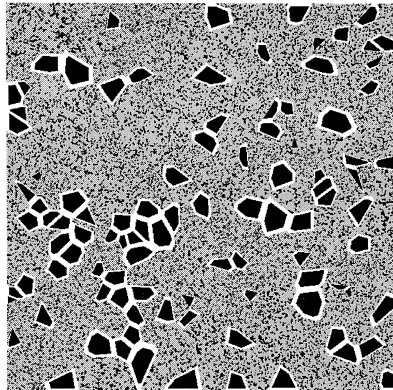
$d = 2, n = 20, z = 0.75, x = y = 0.125, D = 1.904, k = 0.707, i = 2$

Fig. 9. PSF numerically equivalent to the example presented in Fig. 7, with a void phase surrounding the solid.
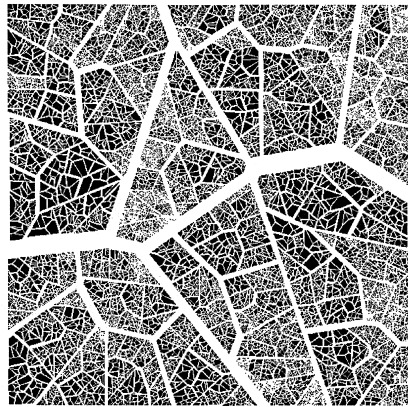
$d = 2, n = 2.65, z = 0.92, x = 0.08, y = 0, D = 1.919, i = 5$

Fig. 10. 2D representation of a random realization of the fractal cube considered by Rieu and Sposito (1991a,b,c), fragmented by a Voronoï tessellation. In this solid mass fractal, the fractal set is associated to the solid phase.

Unfortunately the network of fractures appears excessively connected for modelling a soil pore space.

5. Conclusion

In conclusion, the PSF model originating with Neimark (1989) and Perrier (1994) can be viewed as a fully self-consistent fractal model of general application in the sense that it is not tied to a specific local geometry. Whilst this is equally true of a mass fractal, the generality of a PSF obviously exceeds that of a mass fractal. Mass fractals have already featured prominently in modelling complex porous materials and it remains to be seen to what extent the wider class of PSF models follows this trend.

Neither the pore phase nor the solid phase of a general PSF exhibit mass fractal scaling. On the other hand the pore–solid interface is fractal for $D > d - 1$. At any stage of its development, the PSF can model a two-phase porous structure. When the structure extends ad infinitum, its porosity approaches a finite value that can be chosen by the modeller between the extreme value 0 or 1 independently of the fractal dimension. Finally the main peculiarity of the PSF is the association in the same geometric shape of a distribution of pores and a distribution of solids which both assume a power law form with the same fractal exponent. As a result of this symmetry, the PSF model appears promising in terms of modelling hydraulic properties based on structural properties of the solid phase. If in addition an appropriate geometric shape is used, the connectivity of the pore network can be taken into account in pore network

simulations. Intrinsic to a mass fractal and a PSF model as presented in this paper are the notions of multiscale structure and self-similarity of structure. Further generalization is possible when the latter notion is relaxed. Construction of a model in which similarity of structure at different scales is not required further widens its scope of application. These points will be developed in forthcoming papers.

6. List of symbols

D	fractal dimension
d	Euclidean space dimension
L	linear size of the initiator
N	number of subregions paving the initiator
n	inverse of the similarity ratio
z	proportion of subregions where the whole shape is replicated
x	proportion of subregions kept as pores
y	proportion of subregions kept as solids
$\mathcal{N}_z(r_i)$	total number of replicates of size r_i created at iteration step i
$\mathcal{N}_x(r_i)$	total number of pores of size r_i created at iteration step i
$\mathcal{N}_y(r_i)$	total number of solids of size r_i created at iteration step i
$N_z(r_i)$	total number of replicates of size greater than or equal to r_i
$N_x(r_i)$	total number of pores of size greater than or equal to r_i
$N_y(r_i)$	total number of solids of size greater than or equal to r_i
m	last step of division if any
α	means 'proportional to'
ϕ	porosity
ϕ_i	partial porosity at step i
$B_x(i)$	number of boxes of size r_i needed to cover the pores
$B_y(i)$	number of boxes of size r_i needed to cover the solids
$B_z(i)$	number of boxes of size r_i needed to cover the fractal set
$M_x(i)$	volume (or mass) of pores at iteration step i
$M_y(i)$	volume (or mass) of solids at iteration step i
$S(i)$	area of the pore–solid interface
$S_x(i)$	cumulative boundary of pores at iteration step i
$S_y(i)$	cumulative boundary of solids at iteration step i
$p_x(i)$	probability that an arbitrary chosen point on the solids boundary belongs to the solid–pore interface
$p_y(i)$	probability that an arbitrary chosen point on the pores boundary belongs to the solid–pore interface
k	ratio of the similarity transformation used by Perrier (1994) to define the size of the solids and pores associated to any subregion

Appendix A

A.1. Equivalence between the model of Perrier (1994) and the PSF model

Perrier's model is defined on the basis of three parameters (N, z, k) which are equivalent to the set (N, x, y) defining the PSF model.

Perrier's model involves Nz and $N(1 - z)$ subregions as does the PSF. The parameter k defines the ratio of the contracting similarity used to replace each of the $N(1 - z)$ subregions of linear size r by one solid of volume $k^d r^d$ surrounded by one pore of volume $(1 - k^d)r^d$ (see Figs. 8 and 9). An equivalent PSF model can be created by choosing the same N and the following x and y proportions: $x = (1 - z)(1 - k^d)$, $y = (1 - z)k^d$

Conversely, if a PSF model is defined by the parameters (N, x, y), an equivalent model is obtained using Perrier's definitions by choosing the same N and the following z and k values:

$$z = 1 - x - y, \quad k = \left(\frac{y}{x + y} \right)^{1/d}$$

All the results obtained in this paper could have been also derived using Perrier's definition. For instance, the equivalent of the total porosity given in Eq. (20), $\phi = x/(x + y)$, is: $1 - k^d$. Limiting cases $x = 0$ and $y = 0$ correspond respectively to $k = 1$ and $k = 0$.

References

Ahl, C., Niemeyer, J., 1989. The fractal dimension of the pore volume inside soils. Z. Pflanzen-ernährungu. Bodenkunde 152, 457–458.

Arya, L.M., Paris, J.F., 1981. A physico-empirical model to predict the soil moisture characteristic from particle-size distribution and bulk density data. Soil Sci. Soc. Am. J. 45, 1023–1030.

Bartoli, F., Philippy, R., Doirisse, M., Niquet, S., Dubuit, M., 1991. Silty and sandy soil structure and self-similarity: the fractal approach. J. Soil Sci. 42, 167–185.

Bird, N., Bartoli, F., Dexter, A.R., 1996. Water retention models for fractal soil structures. Eur. J. Soil Sci. 47, 1–6.

Crawford, J.W., 1994. The relationship between structure and the hydraulic conductivity of soils. Eur. J. Soil Sci. 45, 493–502.

Crawford, J.W., Sleeman, B.D., Young, I.M., 1993. On the relation between number–size distributions and the fractal dimensions of aggregates. J. Soil Sci. 44, 555–565.

Crawford, J.W., Matsui, N., Young, I.M., 1995. The relation between the moisture release curve and the structure of soil. Eur. J. Soil Sci. 46, 369–375.

Davis, H.T., 1989. On the fractal character of the porosity of natural sandstone. Europhys. Lett. 8, 629–632.

de Gennes, P.G., 1985. Partial filling of a fractal structure by a wetting fluid. In: Adler, D., et al. (Eds.), Physics of Disordered Materials, Plenum, New York, NY, pp. 227–241.

Friesen, W.I., Mikula, R.J., 1987. Fractal dimensions of coal particles. J. Colloid Interf. 120, 263–271.

Ghilardi, P., Kaikai, A., Menduni, G., 1993. Self-similar heterogeneity in granular porous media at the representative elementary volume scale. Water Resour. Res. 29, 1205–1215.

Haverkamp, R., Parlange, J.Y., 1986. Predicting the water retention curve from particle-size distribution: sandy soils without organic matter. Soil Sci. 142, 325–339.

Katz, A.J., Thompson, A.H., 1985. Fractal sandstones pores: implication for conductivity and pore formation. Phys. Rev. Lett. 54 (12), 1325–1328.

Neimark, A.V., 1989. Multiscale percolation systems. Sov. Phys.-JETP 69, 786–791.

Mandelbrot, B.B., 1983. The Fractal Geometry of Nature. Freeman, San Francisco.

Perfect, E., Kay, B.D., 1991. Fractal theory applied to soil aggregation. Soil Sci. Soc. Am. J. 55, 1552–1558.

Perrier, E., 1994. Structure géométrique et fonctionnement hydrique des sols. Simulations exploratoires. Thèse Université Paris VI (Ed. Orstom, Paris, 1995).

Perrier, E., Mullon, C., Rieu, M., de Marsily, G., 1995. A computer construction of fractal soil structures. Simulation of their hydraulic and shrinkage properties. Water Resour. Res. 31, 2927–2943.

Perrier, E., Rieu, M., Sposito, G., de Marsily, G., 1996. A computer model of the water retention curve for soils with a fractal pore size distribution. Water Resour. Res. 32, 3025–3031.

Pfeifer, P., Avnir, D., 1983. Chemistry in non integer dimensions between two and three: I. Fractal theory of heterogeneous surfaces. J. Chem. Phys. 79, 3558–3564.

Rieu, M., Perrier, E., 1997. Fractal models of fragmented and aggregated soils, In: Baveye, P., et al. (Eds.), Fractals in Soil Science. CRC Press, Boca Raton, FL, pp. 169–202.

Rieu, M., Sposito, G., 1991a. Fractal fragmentation, soil porosity, and soil water properties: I. Theory. Soil Sci. Soc. Am. J. 55, 1231–1238.

Rieu, M., Sposito, G., 1991b. Fractal fragmentation, soil porosity, and soil water properties: II. Applications. Soil Sci. Soc. Am. J. 55, 1239–1244.

Rieu, M., Sposito, G., 1991c. Relation pression capillaire-teneur en eau dans les milieux poreux fragmentés et identification du caractère fractal de la structure des sols. C.R. Acad. Sci., Ser. II 312, 1483–1489.

Toledo, P.G., Novy, R.A., Davis, H.T., Scriven, L.E., 1990. Hydraulic conductivity of porous media at low water content. Soil Sci. Soc. Am. J. 54, 673–679.

Tyler, S.W., Wheatcraft, S.W., 1989. Application of fractal mathematics to soil water retention estimation. Soil Sci. Soc. Am. J. 53, 987–996.

Tyler, S.W., Wheatcraft, S.W., 1990. Fractal processes in soil water retention. Water Resour. Res. 26, 1047–1054.

Tyler, S.W., Wheatcraft, S.W., 1992. Fractal scaling of soil particle-size distributions: analysis and limitations. Soil Sci. Soc. Am. J. 56, 362–369.

van Damme, H., Ben Ohoud, M., 1990. From flow to fracture and fragmentation in colloidal media. In: Disorder and Fracture, NATO ASI Series. Plenum, New York, pp. 105–116.

Wu, Q., Borkovec, M., Sticher, H., 1993. On particle-size distributions in soils. Soil Sci. Soc. Am. J. 57, 883–890.

Young, I.M., Crawford, J.W., 1991. The fractal structure of soil aggregates: its measurement and interpretation. J. Soil Sci. 42, 187–192.